INTERNATIONAL JOURNAL OF
COASTAL & OFFSHORE ENGINEERING IJCOE Vol.3 /No. 4/Winter 2018 (27-35)

Available online at: http://ijcoe.org/browse.php?a_code=A-10-52-1&sid=1&slc_lang=en

Numerical Modeling of Heat and Brine Discharge near Qeshm Desalination Plant

Saeed Memari[1], Seyed Mostafa Siadatmousavi[2*]

[1] M.Sc. Student, School of Civil and Environmental Engineering, Iran University of Science and Technology; s_memari@civileng.iust.ac.ir
[2] Assistant Professor, School of Civil and Environmental Engineering, Iran University of Science and Technology; siadatmousavi@iust.ac.ir*

ARTICLE INFO

Article History:
Received: 26 Dec. 2017
Accepted: 17 Mar. 2018

Keywords:
Numerical Modeling
Desalination Plant
FVCOM
Finite Volume
3D Circulation model

ABSTRACT

Desalination plants have become invaluable solutions especially where freshwater resources are scarce. However, the byproduct of their operation is an outflow which is more saline and heated than the ambient water body. This heated plume adversely affects the ecosystem if it is not treated properly. In this study, 3D finite volume coastal and ocean model is employed to address this issue close to Qeshm Island. In addition to calibrating the model, two alternatives are simulated and discussed to mitigate the adverse effects of the heated plume. It is shown that the plume tends to move in the upper layer of the water column due to its lower density than the ambient water. By moving the outfall to deeper parts of the sea—10-meter-deep—the negative effects of the plume significantly decrease, and as a result, it fulfills the Iran national guidelines. Moreover, due to the mechanism of the Qeshm desalination plant, the spread of salinity is of the least importance compared to the increase in temperature.

1. Introduction

Today, with the galloping rate of water use in both industrial and municipals sectors, the need for a reliable source to this end is crucial. Meanwhile, desalination plants have become invaluable tools to supply freshwater; however, their byproduct – brine – should be accurately dealt with, since the brine can adversely affect the environment if it is not discharged appropriately and according to guidelines [1]. The Qeshm desalination plant is located at the northern part of the Qeshm Island. It uses distillation process to extract freshwater from oceanic saline water. However, by using this process, the outflow is not only more saline than the ambient water—sea water—but also warmer due to the process it went through. Warm and saline water discharged into the sea adversely affects fauna and flora close to the outfall location [2]. Accordingly, especial discharge plan should be considered to deal with this kind of byproduct.

Two types of approaches are employed when discharging into the sea is concerned [3], first of which is near-field approach which deals with the area where the plume is greatly dominated by the momentum force. This momentum is generated when the brine leaves the outfalls, and its effect is much greater than the turbulence existing in the sea. The parameter which is most important in this region is dilution. Physical condition, namely shape, diameter, and the number of outfalls as well as well as ambient conditions, namely depth and currents are of great importance when the plume behavior in the near-field is concerned. The second approach is called far-field, and the far-field area begins where the plume is no longer bounded to the initial momentum of the outfall. In fact, sea currents and sea turbulence are the most important factors in dispersion of the plume in far-field area [4-6].

Among methods to determine the plume behavior, mathematical models are used by solving the advection-diffusion equation under certain conditions to simplify the equation [7]. To solve the equation, its parameters for describing the ambient currents and conditions should be simplified in a way that the equation can be solved analytically [8, 9]. Accordingly, this method is unable to consider all parameters playing roles in dispersion of the plume at the same time. On the other hand, hydrodynamic models have become invaluable tools in simulating the currents and plume behavior using all parameters having impact on currents and plume behavior.

Purnama et al. studied the optimum location of the outfall by solving advection-diffusion equation so that the brine effects at the beach are minimized [7, 10, 11].

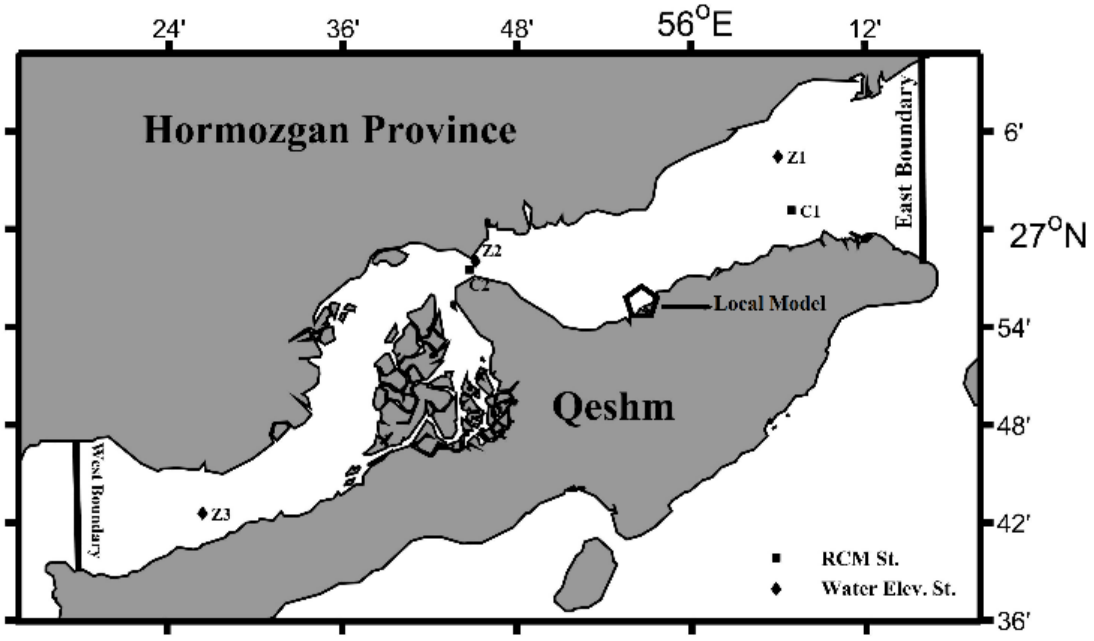

Figure 1: The regional model domain, open boundaries, location of the local model, and the stations used for calibration. The domain of the local model is shown by pentagon.

They solved this equation under simplified condition to determine the horizontal distribution of the brine plume. Similarly, Mohamed used a 2D numerical model to assess the effects of land reclamation on the circulation on the behavior of the heated plume [12]. Likewise, Sun et al. used a 3D numerical model (FVCOM) to determine the plume behavior for a reverse osmosis desalination plant and to locate the outfall where it has minimum effect on the sea grass [13].

2. Materials and Methods

2.1. Case Study

Khuran Channel—also known as Strait of Khuran—is located at the north part of the Persian Gulf (Fig. 1), between Qeshm island and southern mainland of Iran (55.24-56.25 E, 26.60-27.15 N). The maximum depth of the channel is ~34 meters (Fig. 2), and it is considered as a shallow channel [14]. Length of the Khuran Channel between its west and east borders is 110 km, and its maximum width is ~25 km at its east border and its minimum width is ~3.5 km at the middle of the channel. Meteorological data acquired from Iran Meteorological Organization assert that the variation in temperature between day and night are not significant and the weather is considered warm and humid in summers with mild temperature in winters.

Furthermore, current directions are mainly along the channel, and currents are mainly generated by tides. Likewise, main tide constitutes are M2, S2, N2, K1, and O1 [15, 16]. Wind, on the other hand, poorly contributes on the generation of currents, since wind direction is generally perpendicular to dominant alongshore currents induced mainly by tide; therefore, wind effects are negligible [14].

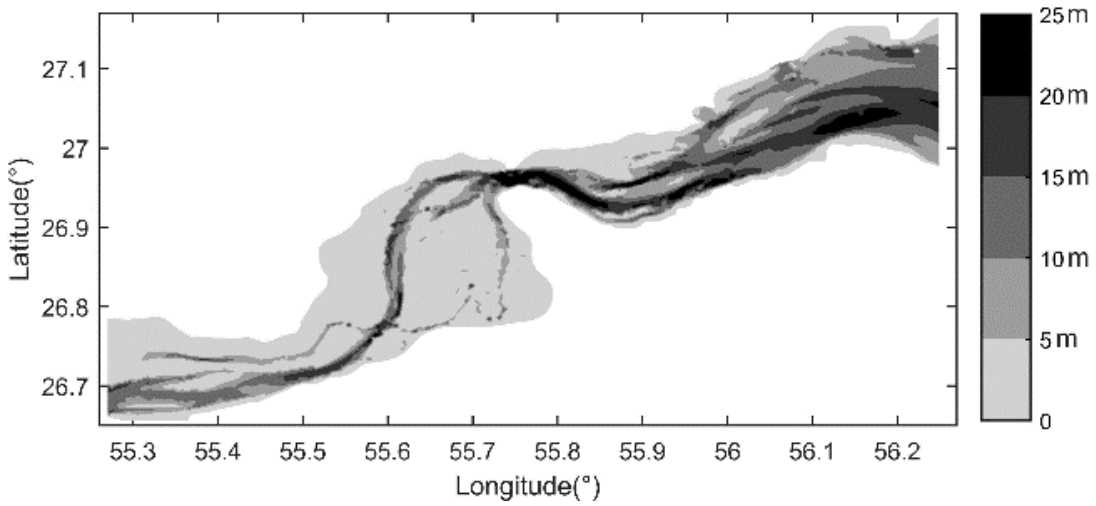

Figure 2: Bathymetry of the Khuran Channel in the northern part of the Qeshm Island

Khuran Channel is the habitat of many marine animals and plants. Moreover, mangrove forests are present in the middle of the channel, and they are preserved as protected areas. There are also a number of industrial facilities along the coast of Khuran Channel, namely ship building companies, power plants, desalination plants, ports, to name but a few. Most of these facilities discharge their waste into the channel. Meanwhile, heated outflows are of great importance, since not only they adversely affect the marine ecosystem, but they might cause stratification as well, taking a great deal of time to dilute with ambient water.

Qeshm desalination plant had experienced some problems in its discharge pipelines and decided to discharge its heated and saline waste through a channel at the beach and on the surface near the plant. By applying this old-fashioned method of discharging, it took a long time for the outflow to dilute because currents near the shore were generally weak. Moreover, the absence of initial momentum existed for a submerged outfall also increased the dilution time.

2.2. Governing Equations and the Numerical Model

Finite Volume Coastal and Ocean Model—FVCOM—with an unstructured grid was applied for this study [17]. FVCOM numerically solves the equations of conservation of momentum, continuity, temperature, salinity, and equation of state for density, analogous to the equations used in other ocean models, which are presented hereunder.

$$\frac{\partial u}{\partial t}+u\frac{\partial u}{\partial x}+v\frac{\partial u}{\partial y}+w\frac{\partial u}{\partial z}-fv=-\frac{1}{\rho_0}\frac{\partial P}{\partial x}\frac{\partial}{\partial z}\left(K_m\frac{\partial u}{\partial z}\right)+F_u \quad (1)$$

$$\frac{\partial v}{\partial t}+u\frac{\partial v}{\partial x}+v\frac{\partial v}{\partial y}+w\frac{\partial v}{\partial z}-fu=-\frac{1}{\rho_0}\frac{\partial P}{\partial y}+\frac{\partial}{\partial z}\left(K_m\frac{\partial v}{\partial z}\right)+F_v \quad (2)$$

$$\frac{\partial P}{\partial z}=-\rho g \quad (3)$$

$$\frac{\partial u}{\partial x}+\frac{\partial v}{\partial y}+\frac{\partial w}{\partial z}=0 \quad (4)$$

$$\frac{\partial T}{\partial t}+u\frac{\partial T}{\partial x}+v\frac{\partial T}{\partial y}+w\frac{\partial T}{\partial z}=\frac{\partial}{\partial z}\left(K_h\frac{\partial T}{\partial z}\right)+F_T \quad (5)$$

$$\frac{\partial S}{\partial t}+u\frac{\partial S}{\partial x}+v\frac{\partial S}{\partial y}+w\frac{\partial S}{\partial z}=\frac{\partial}{\partial z}\left(K_h\frac{\partial S}{\partial z}\right)+F_S \quad (6)$$

$$\rho=\rho(T,S) \quad (7)$$

where x, y, and z are east-west, north-south, and up-down directions at Cartesian coordinate, respectively; similarly, u, v, and w are the velocity components at x, y, and z directions. T, S, ρ, P, f, and g are water temperature, salinity, density, pressure, Coriolis coefficient, and gravity acceleration coefficient. K_m, K_h, F_u, F_v, F_T, and F_s denote the vertical eddy viscosity coefficient, thermal vertical eddy diffusion coefficient, horizontal momentums, thermal diffusion terms, and salt diffusion terms, respectively.

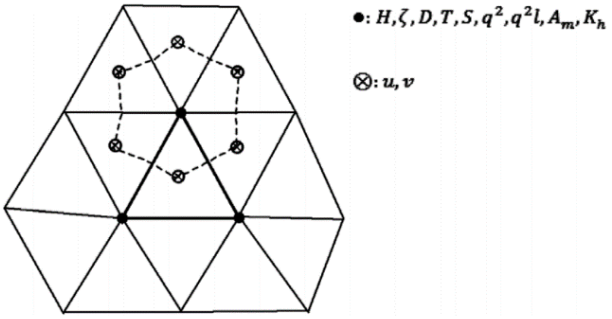

Figure 3: Illustration of triangular unstructured grid. Scalar quantities are defined on the nodes and vectors are defined on the center of elements.

As shown in Fig. 3, the scaler parameters are located on the nodes and the velocity components are located in the center of mesh elements.

Furthermore, the Smagorinsky formula [18] and Mellor and Yamada level 2.5 turbulence closure schemes [19] are used for horizontal viscosity and diffusivity, and vertical mixing.

Using an unstructured triangular grid, FVCOM is capable of modeling complex coastlines and sharp topographies. For vertical layer, σ-coordinate system is used, and at the same time unstructured triangular grid is used for horizontal grid. A finite volume method makes benefit from finite element advantages such as geometric flexibility, and from finite difference advantages namely simple discrete system and effective computation. Thus, the model perfectly functions in describing mass, momentum, and conservation of heat and salt for a complex coastline area.

Furthermore, FVCOM is very capable at calculating wet and dry conditions which makes it an invaluable tool where wet and dry condition is concerned, especially in mangrove forests (Hara Jungle) where it submerged under the water during tidal floods, and it rises above the water during ebb period, making it a dry region. Memari and Siadatmousavi showed that by assuming the Hara Jungles as a wet region at all time or a dry region at all time, currents change dramatically before, after, and at the Jungle regions [20]. Therefore, application of FVCOM nicely suites for this region.

3. Models

3.1. Model Inputs and Description

In the first place, due to the spatially extensive domain, two models with different inputs and mesh sizes are employed: the regional and the local model. The regional model which is the bigger one with courser mesh size is employed to calculate the tide, salinity, and temperature in the Khuran channel, and then provides the boundary conditions for the local model nested inside the regional model.

3.2 Regional Model

The regional model consisted of 10233 elements and 5396 nodes. Moreover, their size near the local model is ~35 meters and grows to ~700 meters at the open

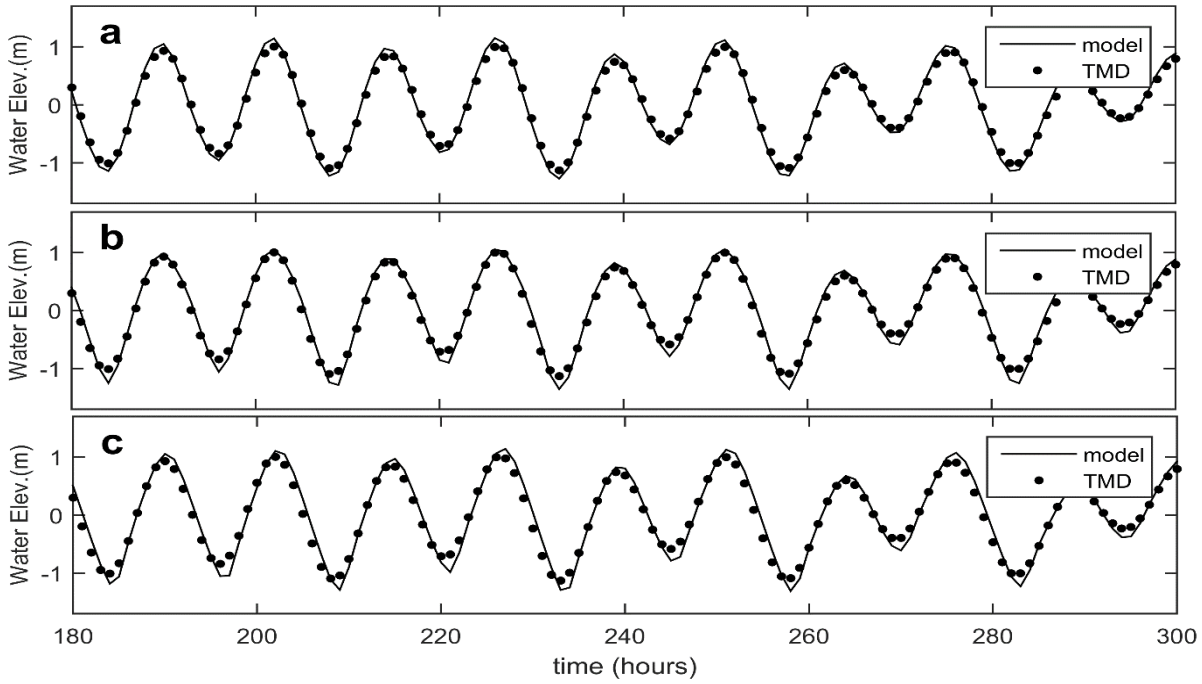

Figure 4: Comparison of tidal elevation and model results at St. Z1 (a), Z2 (b), and Z3 (c).

boundaries, and therefore the elements near the local model boundaries are smaller. The duration of the model run starts from 2005/08/30 to 2005/09/14 for the total of 15 days which includes a full neap and spring tidal cycle. Also, the model startup is set as cold start, and the initial salinity and temperature are set as 32 psu and 32.5°C, respectively. The external time step of the model is set as 0.09 seconds.

The forcing imposed to the model is wind, tide, salinity, and temperature. Wind data are attained from ECMWF Era-Interim database [21] and imposed throughout the domain for the period of the model run. At the same time, although CTD field data showed that the temperature and salinity are vertically homogenous [14], the salinity and temperature data acquired from HYCOM database center [22] are imposed at both east and west open boundaries for the duration of the model run. Furthermore, tide data are attained from TMD model [23] for the duration of the model run at both east and west open boundaries. The harmonic constitutes of tide imposed to the model are $M2, S2, N2, K2, K1, O1$, and $P1$.

Furthermore, bathymetry data used for both regional and local model are acquired from Iran National Cartographic Center [24] with some modification using both GEBCO and local data [25].

3.3. Regional Model Calibration

Bottom roughness coefficient is used to calibrate the model with respect to the five stations assigned along the channel, three of which are used to compare TMD results with model predictions of the water elevation. The other two are RCM9 devices, recording the velocity components of u and v, the locations of which are shown in Fig.1. The data used for stations C1 and C2 were measured by Iranian National Institute for Oceanography and Atmospheric Science in 2005.

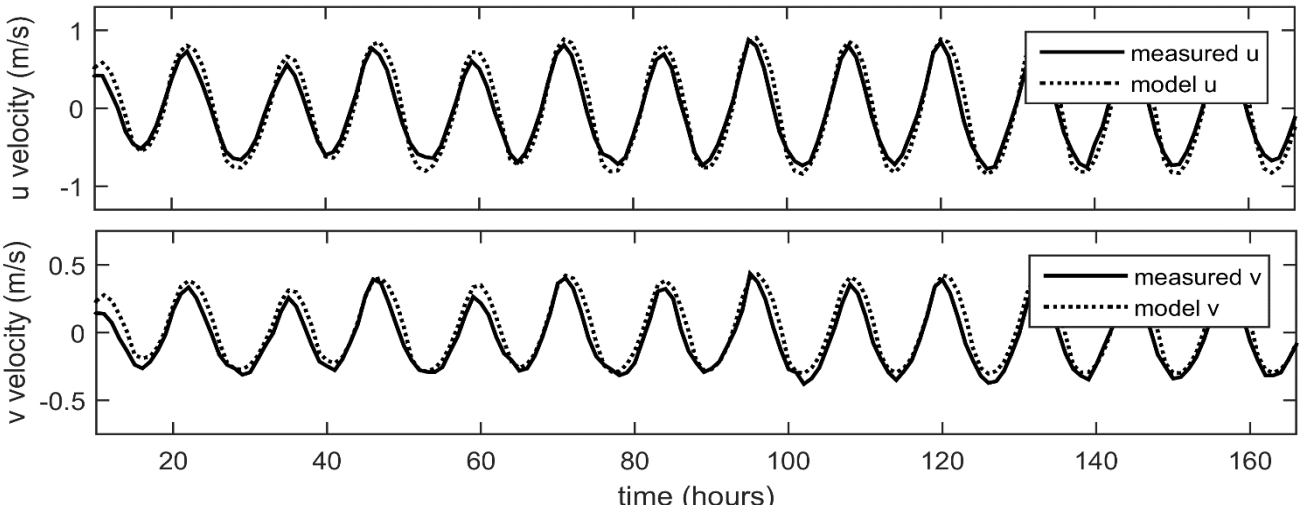

Figure 5: Comparison of velocity between measured data and model results at St. C1

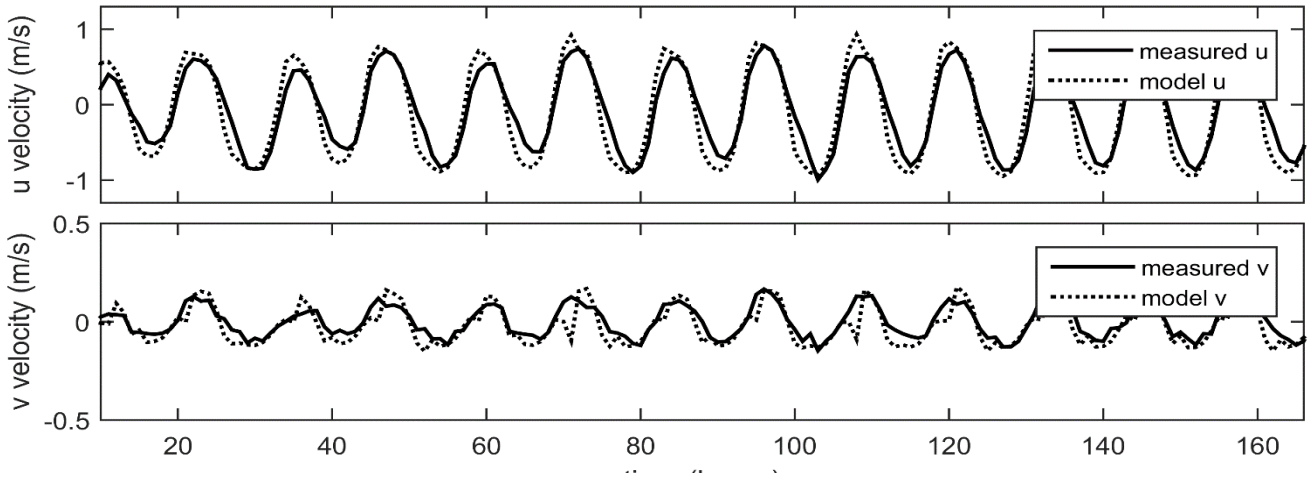

Figure 6: Comparison of velocity between measured data and model results at St. C2

As it can be seen in Fig. 4, the water elevation for all three stations (Z1 to Z3), are in a very good agreement with the TMD results. In similar fashion, in Fig. 5 and 6 the velocity calculated by the regional model and the in situ velocity data are compared, and it can be seen that the two are in a very good accord. Furthermore, the RMSE criterion and the correlation coefficient for all five stations are presented in Table 1, showing that the regional model is well calibrated.

Table 1: RMSE and Correlation Coefficient for all five St.

Station	RMSE	Correlation coef.	Depth (m)
Z1	0.096	0.993	16.65
Z2	0.114	0.990	31.87
Z3	0.130	0.987	16.75
C1	0.150	0.979	21.52
C2	0.218	0.948	28.56
Perfect Match	0	1	---

3.4 Local Model

Since the spread of heat and brine happens in a relatively short distance from the outfall, employing a local model with smaller mesh size is vital. To this end, a local model with a higher resolution consisted of 8848 elements and 4552 nodes is constructed in a way that the minimum mesh size at the outfall locations is 10 meters and increases to 200 meters at the open boundary (Fig. 7). Similarly, the external time step for the local model is set to 0.03 seconds.

Since the dispersion of heat and saline water is greatly affected by horizontal and vertical dispersion coefficient, the local model then should be calibrated with respect to the heat and saline outflow. To this end, four CTD stations at the distance of 150 and 200 meters from the coastal discharge point—present situation—

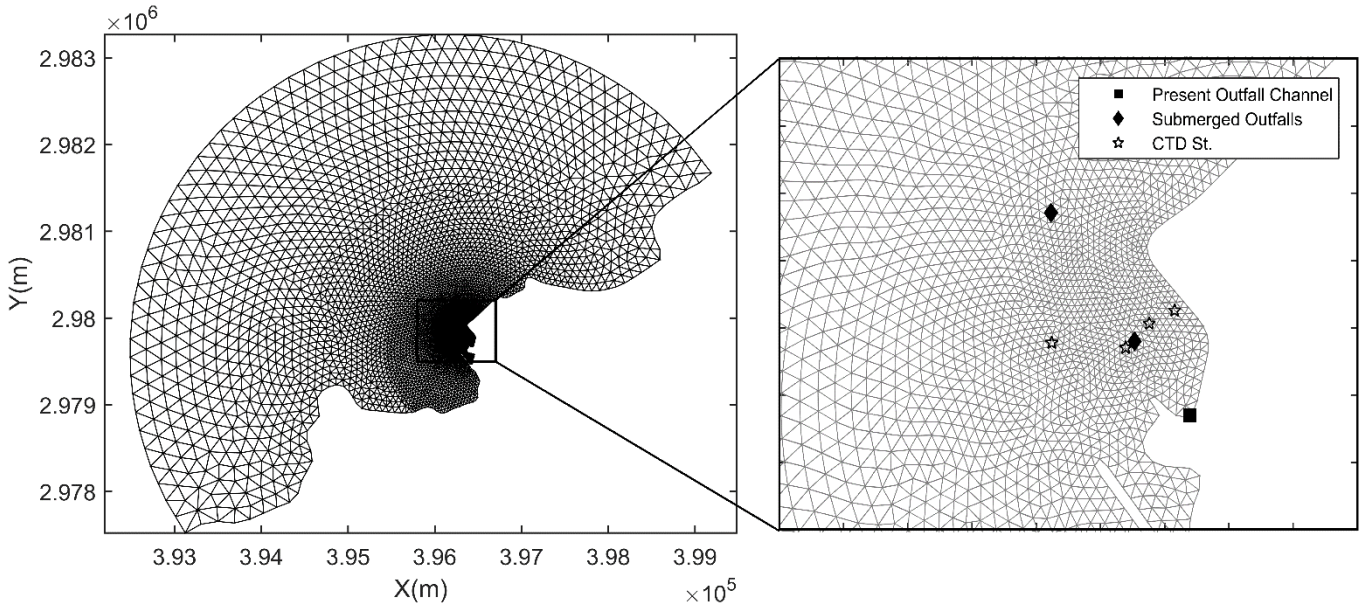

Figure 7: Local model mesh as well as present coastal discharge and submerged scenarios

were used to calibrate the local model with respect to the heat and salinity dispersion.

However, unlike field measurements used for calibrating the hydrodynamics of the regional model, the CTD field measurements were conducted at year 2016. Therefore, the calibrated regional model was run again for that period and the boundary conditions namely salinity, temperature, and tide for the local model was transferred from the regional model to the nested local model. Similarly, the ECMWF wind data were used in the local model as well. The local model was calibrated in a way that the maximum difference of the salinity or heat between the model results and measured results would be less than 4 percent (see Table 2).

Table 2: Maximum error of calibration as well as distance of the CTD Stations from the present discharge channel

Station	t82	t32	t92	t4
Maximum Abs. Error (℃)	0.432	0.796	0.449	0.837
Maximum Percent Error (%)	1.90	3.50	2.03	3.90
Distance From Outfall (m)	150	150	150	200

An extra day is added to the simulation period to warm up the model for velocities, tides, salinity, and temperature. Moreover, the actual discharge point of the outflow, an open channel at the shoreline, is implemented with discharging rate of 2.5 m^3/s, and the temperature and salinity of 31℃ and 43 psu, respectively, according to the CTD field data at the mouth of the discharge channel. Similarly, the initial values of water salinity and temperature are set as 37.4 psu and 21℃, respectively.

Furthermore, to assess the permissible amount of heat and salinity, different countries have distinct guidelines and regulation based on their native ecosystem. According to Iran national regulation, the maximum amount of temperature at the distance of 200 meters from the outfall must not exceed 3℃ from the ambient water temperature. Similarly, the maximum amount of salinity must not exceed 10% of the ambient water salinity.

4. Distribution of Heat and Saline Outflow

The outflow whose temperature is above the ambient water tends to float and move at the upper layer of water column, and at the same time, the outflow which is more saline than the ambient water tends to sink and move close to the bottom of sea. In this case which is a combination of saline and heated water, the outflow tends to move in upper layer due to the dominant effect of heat on the density of the plume compared to corresponding effect by salinity [26].

As it was mentioned before, three cases are discussed in this study, first of which is the actual method of discharging—surface discharge through a channel at the beach—and two other scenarios which are submerged outfalls, a 5.5-meter-depth and 10-meter-depth submerged outfalls.

4.1. Distribution of Heat

Fig. 8 shows the maximum amount of excess heat at the distance of 200 meters from the present outfall as well as other scenarios for all time steps during the local model run. In each time step during the local model run (one day), the greatest value of heat is depicted, and as it can be seen, for the present outfall—surface discharge—almost in all time steps, the value of heat outreached the guidelines—the horizontal line showing the value of 3 (in degrees Celsius). As the outfall moved to deep areas of the sea and also changed the mechanism of discharging from surface discharge to submerged discharge, the critical value of heat decreased dramatically. Moreover, having moved the outfall to 10-meter-depth, the results asserts that due to the high speed currents, depth, turbulence, and more dilution, the maximum amount of heat in each time step decreased dramatically, showing that it is the best place

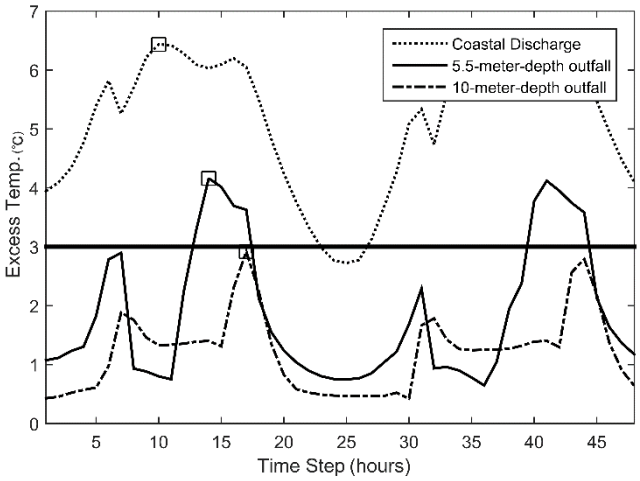

Figure 8: Maximum amount of increase in temperature at the distance of 200 meters from the outfall location for all scenarios and time steps

to discharge the outflow.

Fig. 9 shows the horizontal dispersion of heat at the upper layer of the water column in critical time steps marked on Fig. 8 by squares. As it can be seen, the coastal discharge is the worst method of discharge, causing the plume to slowly dilute, and therefore vast area of the sea is affected by excess heat. The 5.5-meter-deep outfall dilute the plume with much faster rate than the coastal discharge; However, it fails to satisfy guidelines, stating that the amount of excess heat at the 200-meter distance from the outfall must be less than 3℃. Finally, the 10-meter-deep submerged outfall is capable of generating enough dilution for the

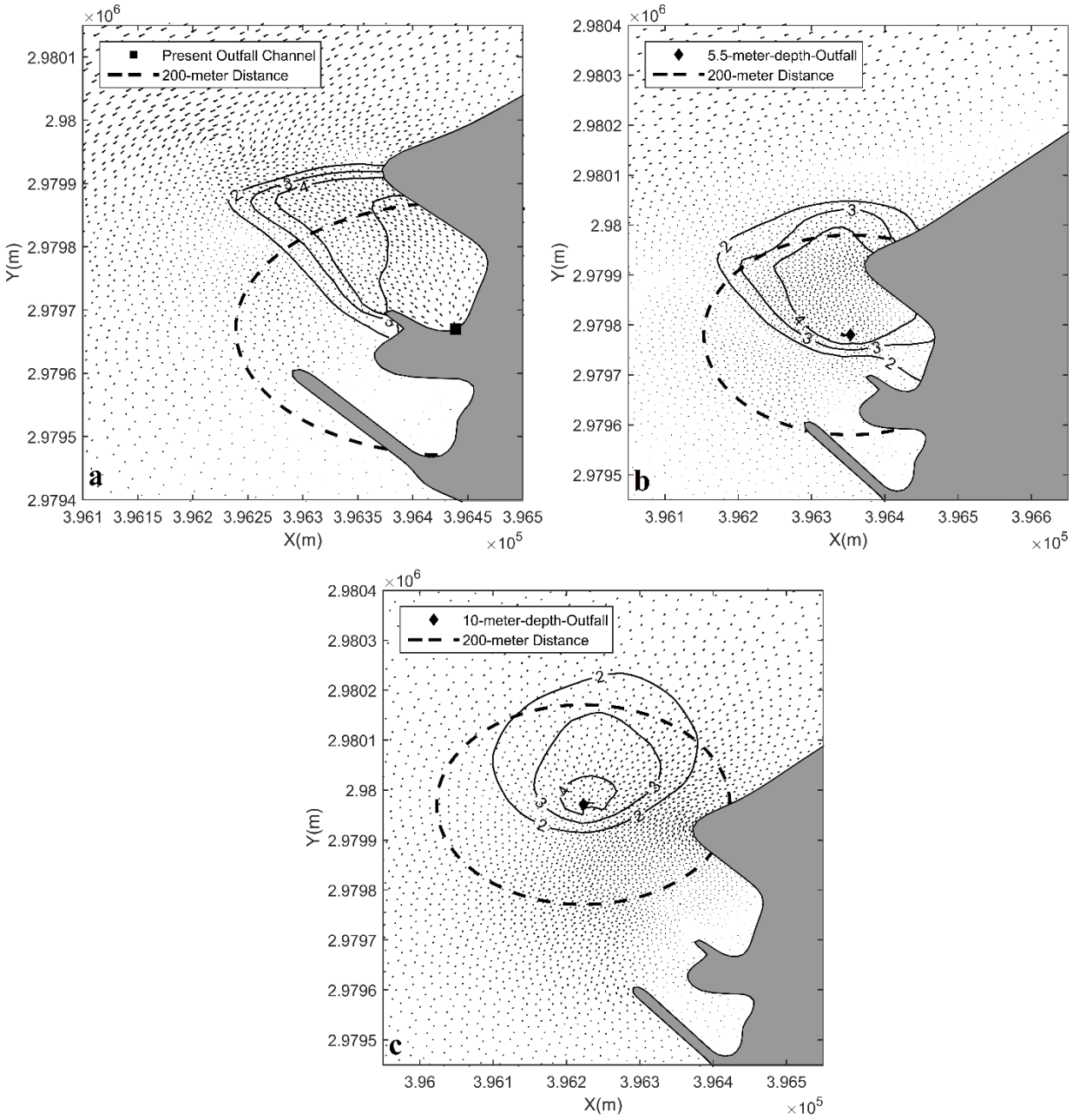

Figure 9: Surface dispersion of heat for (a) surface discharge, (b) 5.5-meter submerged outfall, and (c) 10-meter submerged outfall. The corresponding current vectors for the upper layer are also demonstrated

plume to leave the excess heat of less than 3℃ at 200-meter distance from the outfall location. Therefore, only 10-meter-deep outfall is capable of maintaining the guidelines in all time. Note that the rise and fall in the time series of temperature is in fact out of phase with tidal current; i.e. when current speed is low, the temperature rise is higher due to lack of advection which helps to dilute the plume with the ambient water. Fig. 10 shows the critical situation of heat dispersion when water elevation is at high value. In the absent of a strong current, more time is needed for the plume to dilute with ambient water. Therefore, the two high peaks for each line in Fig. 8 correspond to the high and the low water elevation, or in other words weak currents (slack water).

4.2. Distribution of Salinity

The regulations assert that the amount of salinity at the distance of 200 meters from the outfall should be less than 10% of the background salinity—in this case it equals to 3.75 psu. Since the mechanism in which the power plant turns the saline water into fresh water is of distillation kind, the amount of salinity of the outflow does not dramatically increase. As it can be seen for the worst case in Figure 10, which is the surface discharge, the amount of salinity change at the 200-meter distance hardly reaches the amount of 3 psu. Therefore, for other scenarios, the change in salinity distribution is not presented.

5. Conclusion

In this study, a three-dimensional finite volume circulation model was employed to study the dilution

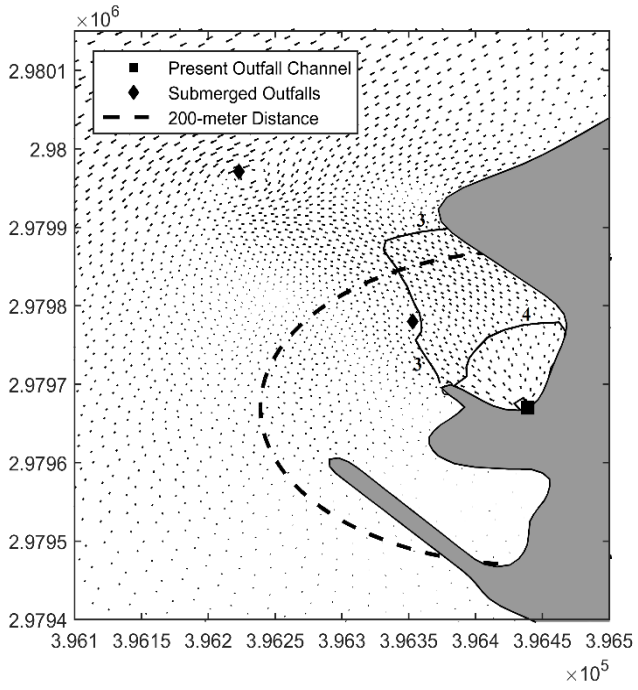

Figure 10: Salinity dispersion from surface discharge point

of outflow from a power plant with ambient water body. This invaluable tool enables us to easily model the current situation to not only better understand the circulation pattern but also plan for the optimum way of discharging.

After calibrating the far-field model based on water elevation and current speed, a local model with smaller mesh size was employed, then temperature, salinity, tide, and wind were nested into the local model. Local model was then calibrated using the CTD field data to determine horizontal mixing coefficient with respect to the actual discharging method—surface discharge. Calibrating the local model, two scenarios were used with respect to both depth and currents. Moreover, discharging method altered to submerged one to better dilute the outflow.

It was shown that by moving the outfall location to deeper areas of the sea where tidal currents are stronger, the dilution rate increases, and therefore the plume disperse more quickly. However, when the regulation guidelines are concerned, only the 10-meter-outfall can be applied.

Salinity, on the other hand, is of the least importance, since the process of producing fresh water—in this case—makes the outflow with only a little extra amount of salt compared to the ambient salinity level.

6. References

1- Ahmad, N., & Baddour, R. E., (2014), *A review of sources, effects, disposal methods, and regulations of brine into marine environments*, Journal of Ocean & coastal management, 87, 1-7.

2- Anschutz, P., Blanc, G., Chatin, F., Geiller, M., & Pierret, M.-C., (1999), *Hydrographic changes during 20 years in the brine-filled basins of the Red Sea*, Journal of Deep Sea Research Part I: Oceanographic Research Papers, 46(10), 1779-1792.

3- Niepelt, A., Bleninger, T., & Jirka, G., (2008), *Desalination brine discharge modelling. Coupling of hydrodynamic models for brine discharge analysis*, Paper presented at the 5th International Conference on Marine Waste Water Discharges and Coastal Environment, Croatia.

4- Fischer, H. B., List, J. E., Koh, C. R., Imberger, J., & Brooks, N. H., (2013), *Mixing in inland and coastal waters*: Elsevier.

5- Grace, R. A., (1978), *Marine outfall systems: planning, design, and construction*: Prentice-Hall.

6- Sharp, J. J., (1989), *Discussion of "Initial Dilution of Horizontal Jet in Crossflow" by Joseph HW Lee and Peter Neville-Jones (May, 1987, Vol. 113, No. 5)*, Journal of Hydraulic Engineering, 115(2), 282-284.

7- Purnama, A., & Al-Barwani, H., (2006), *Spreading of brine waste discharges into the Gulf of Oman*, Journal of Desalination, 195(1-3), 26-31.

8- Kay, A., (1997), *Advection-diffusion in reversing and oscillating flows: 2. Flows with multiple reversals*, IMA journal of applied mathematics, 58(3), 185-210.

9- Macdonald, G. J., & Weisman, R. N., (1977), *Oxygen-sag in a tidal river*, Journal of the Environmental Engineering Division, 103(3), 473-488.

10- Purnalna, A., Al-Barwani, H., & Al-Lawatia, M., (2003), *Modeling dispersion of brine waste discharges from a coastal desalination plant*, Journal of Desalination, 155(1), 41-47.

11- Purnama, A., & Shao, D., (2015), *Modeling brine discharge dispersion from two adjacent desalination outfalls in coastal waters* Journal of Desalination, 362, 68-73.

12- Mohamed, K. A., (2007), *Model investigation on the impact of raha beach development on Umm Al Nar Power and Desalination Plant*, Journal of Desalination, 212(1-3), 357-366.

13- Sun, Y.-J., Cho, Y.-K., Park, K.-S., Yoon, S.-M., & Moon, J.-K., (2012), *Simulation of brine discharge near sea farms in the Korea Strait*, Journal of Desalination and Water Treatment, 43(1-3), 201-211.

14- Mahmoudov, M., Chegini, V., & Montazeri Namin, M., (2011), *Three-Dimensional Simulation of Qeshm Channel Currents*, Journal of Persian Gulf, 2(3), 9-16.

15- Foreman, M. G. G., (1979), *Manual for tidal heights analysis and prediction: Institute of Ocean Sciences*, Patricia Bay.

16- Najafi, H. S., & Noye, B. J., (1997), *Modelling tides in the Persian Gulf using dynamic nesting.*

17- Chen, C., Liu, H., & Beardsley, R. C., (2003), *An unstructured grid, finite-volume, three-dimensional, primitive equations ocean model: application to coastal ocean and estuaries.* Journal of atmospheric and oceanic technology, 20(1), 159-186.

18- Smagorinsky, J., (1963), *General circulation experiments with the primitive equations: I. The basic experiment.* Monthly weather review, 91(3), 99-164.

19- Mellor, G. L., & Yamada, T., (1982), *Development of a turbulence closure model for geophysical fluid problems.* Reviews of Geophysics, 20(4), 851-875.
20- Memari, S., & Siadatmousavi, S. M., (2017), *Modeling the effects on mangrove forests on hydrodynamics of the Khuran Channel*. 19th Marine Industries Conference, Kish, Iran.
21- https://www.ecmwf.int/
22- https://hycom.org/
23- Padman, Laurie, and S. Erofeeva., (2005), *Tide Model Driver (TMD) Manual*. Earth and Space Research.
24- http://www.ncc.org.ir/
25- https://www.gebco.net/
26- Salgueiro, D., de Pablo, H., Nevesa, R., & Mateus, M., (2015), *Modelling the thermal effluent of a near coast power plant (Sines, Portugal).* Revista de Gestão Costeira Integrada-Journal of Integrated Coastal Zone Management, 15(4).